Cell Metabolism, Volume *34*

Supplemental information

Carbon source availability drives nutrient utilization in CD8$^+$ T cells

Irem Kaymak, Katarzyna M. Luda, Lauren R. Duimstra, Eric H. Ma, Joseph Longo, Michael S. Dahabieh, Brandon Faubert, Brandon M. Oswald, McLane J. Watson, Susan M. Kitchen-Goosen, Lisa M. DeCamp, Shelby E. Compton, Zhen Fu, Ralph J. DeBerardinis, Kelsey S. Williams, Ryan D. Sheldon, and Russell G. Jones

Supplemental Information

Carbon source availability drives nutrient utilization in CD8$^+$ T cells

Irem Kaymak, Katarzyna M. Luda, Lauren R. Duimstra, Eric H. Ma, Joseph Longo, Michael S. Dahabieh, Brandon Faubert, Brandon M. Oswald, McLane J. Watson, Susan M. Kitchen-Goosen, Lisa M. DeCamp, Shelby E. Compton, Zhen Fu, Ralph J. DeBerardinis, Kelsey S. Williams, Ryan D. Sheldon, and Russell G. Jones

Inventory of Supplemental Information

Supplemental Tables

Table S1, related to Figure 1. Summary of metabolite concentrations in medium formulations and mouse and human plasma.

Supplemental Figures

Figure S1, Related to Figure 1. Impact of PCS on $CD8^+$ T cell intracellular metabolite abundance and extracellular nutrient levels.

Figure S2, Related to Figure 2. Impact of media formulations and PCS on $CD8^+$ T cell mRNA expression.

Figure S3, Related to Figure 3. Contribution of extracellular citrate, pyruvate, and alanine to TCA cycle metabolism in $CD8^+$ T cells.

Figure S4, Related to Figure 4. Physiologic carbon sources influence T cell survival and effector function.

Figure S5, Related to Figure 5. Impact of exogenous lactate on $CD8^+$ T cell proliferation, IFN-γ production, and metabolism.

Figure S6, Related to Figure 6. Validation of Ldha silencing in $CD8^+$ T cells.

Table S1, related to Figure 1. Summary of metabolite concentrations in medium formulations and mouse and human plasma.

	IMDM	VIM	RPMI	PCS	Mouse plasma[1,2]	Mouse plasma[3]	Human Plasma[3]
D-Glucose	25000	5000	11111		8333±1966	4380±90	4817±421
L-Alanine	280	200	-		196±16	690±112	448±127
L-Arginine	400	400	1149		93±4	66±13	109±46
L-Asparagine	190	190	378		36±2	50±12	48±18
L-Aspartic acid	230	10	150		13±2	7.0±0.6	21±1
L-Cystine 2HCl	290	290	208		26±4	30±2	101±22
L-Glutamic acid	510	20	136		25±1	19±2	68±46
L-Glutamine	6000*	500	6055*		397±10	934±107	550±62
Glycine	400	100	133		120±4	217 ± 40	266±50
L-Histidine HCl•H_20	200	200	97		50±3	76±12	106±29
L-Isoleucine	800	800	382		73±1	138±9	69±13
L-Leucine	800	800	382		124±21	270±23	158±58
L-Lysine HCl	800	800	219		309±26	176±28	236±111
L-Methionine	200	40	101		52±1	53±5	29±3
L-Phenylalanine	400	400	91		54±3	96±24	79±40
L-Proline	350	350	174		67±1	71±13	190±30
L-Serine	400	100	286		82±2	96±24	141±46
L-Threonine	800	100	168		126±1	145±15	155±55
L-Tryptophan	800	80	25		46±1	62±4	54±14
L-Tyrosine	460	460	111		47±3	69±19	89±42
L-Valine	800	800	171		178±19	262±14	235±25
L-Hydroxyproline	-	-	150		20±3	3.1±0.5	15±4
Acetate				400	433±115	-	36±8
bHB				850	302±108	849 ± 126	53±28
Citrate				215	345±56	214±7	131±53
Lactate				3000	2515±218	3088 ± 431	1640±776
Pyruvate				150	108±14	150±25	61±11

Shown is a summary of major metabolite concentrations in synthetic medium (IMDM, VIM) and physiologic carbon sources (PCS) used in this study. RPMI is included for

comparison. Corresponding metabolite concentrations in mouse plasma[1–3] and human plasma[3] are shown for comparison. Metabolites not included in medium formulations are indicated by (-). All concentrations are listed in μM.

*IMDM and RPMI medium formulations contain 2000 and 2055 μM glutamine, respectively, but are supplemented with 4000 μM glutamine. Glutamine concentrations in final medium formulations are listed.

[1]Sugimoto *et al.*, *Nucleic Acids Research*, 2012; [2]Hui *et al.*, *Nature*, 2017; [3]Cantor *et al.*, *Cell*, 2017.

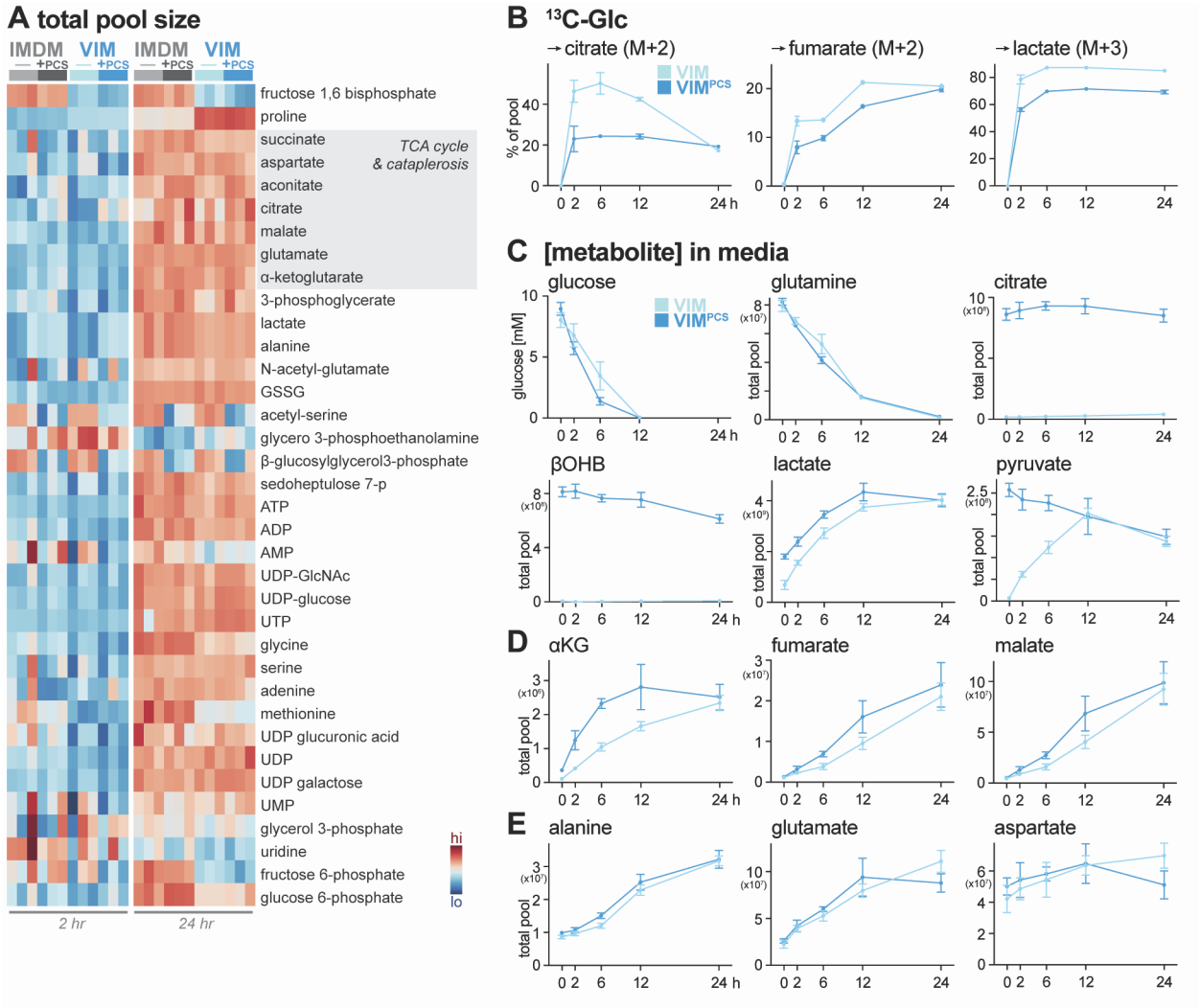

Figure S1, Related to Figure 1. Impact of PCS on CD8⁺ T cell intracellular metabolite abundance and extracellular nutrient levels.

A, Heatmap depicting relative pool size of intracellular metabolites from CD8⁺ T cells cultured in IMDM or VIM with (+) or without (-) PCS from **Figure 1B**. Activated CD8⁺ T cells were cultured in the indicated medium (containing [U-^{13}C]-glucose) for 2 h or 24 h prior to metabolite extraction (mean±SEM, n=3/sample). **B,** Line graphs depicting fractional enrichment of intracellular ^{13}C-glucose-derived citrate M+2, fumarate M+2, and lactate M+3 in activated CD8⁺ T cells over time. Activated CD8⁺ T cells were cultured in VIM (±PCS) containing [U-^{13}C]-glucose for up to 24 h, with intracellular

metabolites extracted at the indicated time points (mean±SEM, n=3/sample). **C–E,** Line graphs depicting extracellular metabolite levels in culture medium over time. Activated $CD8^+$ T cells were cultured in VIM (±PCS) for up to 24 h, and metabolite abundances in extracellular medium were measured at the indicated times (mean±SEM, n=3/sample). Abundances for glucose, glutamine, and PCS (**C**), TCA cycle intermediates (**D**), and amino acids (**E**) are shown.

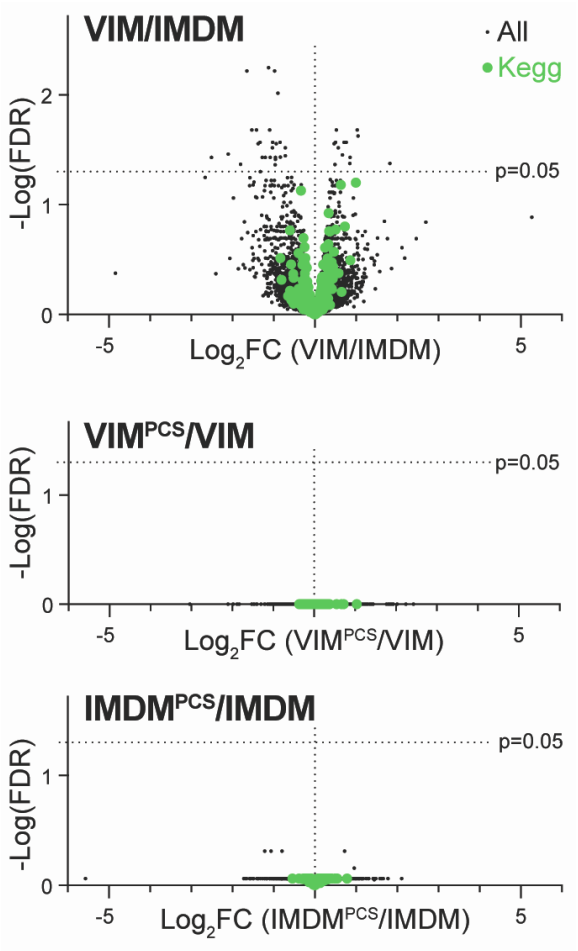

Figure S2, Related to Figure 2. Impact of media formulations and PCS on CD8⁺ T cell mRNA expression.

Volcano plots comparing mRNA expression (Log_2FC) versus statistical significance (-Log(FDR)) for CD8⁺ T cells cultured in VIM versus IMDM (*top*), VIM containing PCS (VIM^{PCS}) versus VIM (*middle*), or IMDM containing PCS ($IMDM^{PCS}$) versus IMDM (*bottom*) for 24 h (corresponding to **Figure 1B**). All genes quantified by RNA sequencing are represented by the black dots, with KEGG metabolism genes highlighted in green. Statistical cutoff at $p<0.05$ is indicated by the dotted line.

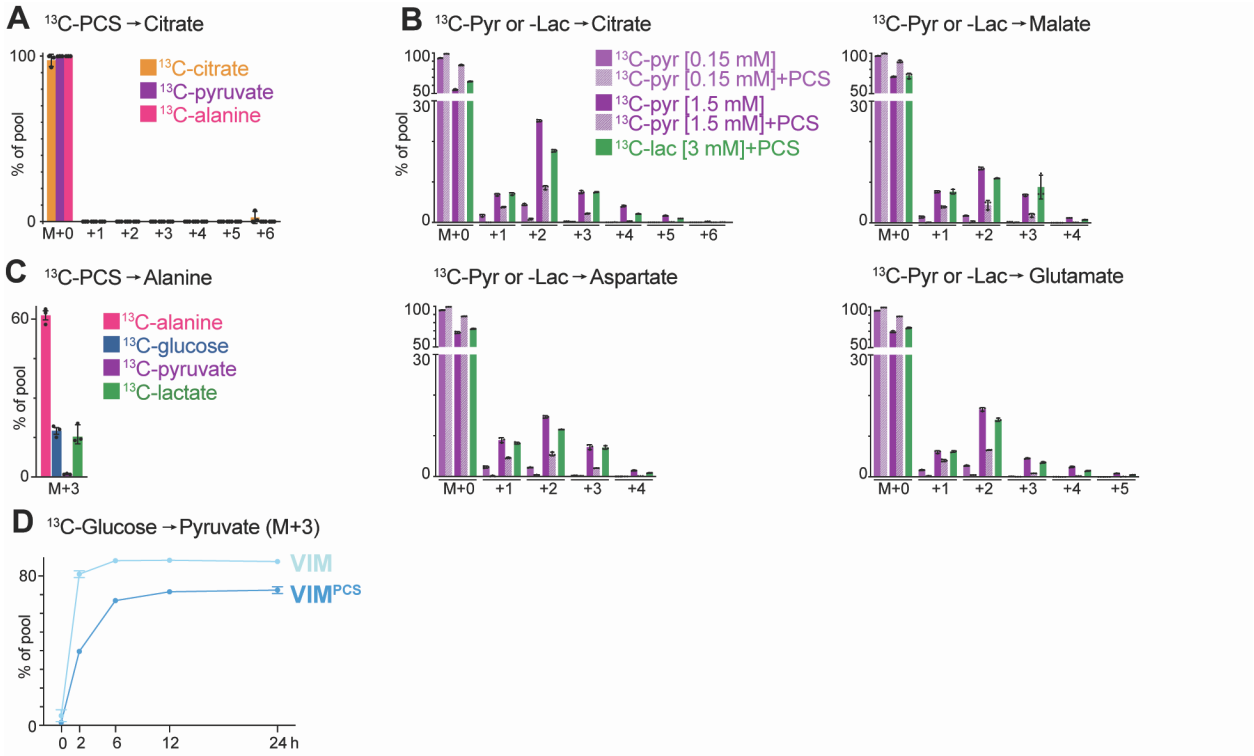

Figure S3, Related to Figure 3. Contribution of extracellular citrate, pyruvate, and alanine to TCA cycle metabolism in CD8⁺ T cells.

A, Bar graph depicting mass isotopologue distributions (MIDs) for [U-^{13}C]-PCS-derived carbon into intracellular citrate for CD8⁺ T cells cultured as in **Figure 3B**. Shown are individual isotopologues derived from [U-^{13}C]-citrate (orange), [U-^{13}C]-pyruvate (purple), or [U-^{13}C]-alanine (pink) after 24 h of culture (mean±SEM, n=3/group). **B,** Bar graphs depicting MIDs for [U-^{13}C]-pyruvate- or [U-^{13}C]-lactate-derived intracellular citrate, malate, aspartate, or glutamate in CD8⁺ T cells. CD8⁺ T cells were stimulated for 3 days in standard IMDM using plate-bound anti-CD3 and -CD28 antibodies, after which activated CD8⁺ T cells were cultured for 6 h in VIM containing physiological (0.15 mM) or high levels (1.5 mM) of [U-^{13}C]-pyruvate in the presence or absence of other PCS (acetate, βOHB, citrate, lactate) at their physiological concentrations (as in **Figure 1A**). Activated CD8⁺ T cells were cultured in VIM plus PCS containing [U-^{13}C]-lactate as a

control (mean±SEM, n=3/group). **C,** Bar graph depicting MIDs for [U-^{13}C]-PCS-derived carbon into intracellular alanine for CD8^{+} T cells cultured as in **Figure 3B**. Shown are individual isotopologues derived from [U-^{13}C]-alanine (pink), [U-^{13}C]-glucose (blue), [U-^{13}C]-pyruvate (purple), or [U-^{13}C]-lactate (green) after 24 h of culture (mean±SEM, n=3/group). **D,** Line graph depicting fractional enrichment of intracellular ^{13}C-glucose-derived pyruvate M+3 in activated CD8^{+} T cells over time. Activated CD8^{+} T cells were cultured in VIM (±PCS) containing [U-^{13}C]-glucose for up to 24 h, with intracellular metabolites extracted at the indicated time points (mean±SEM, n=3/sample).

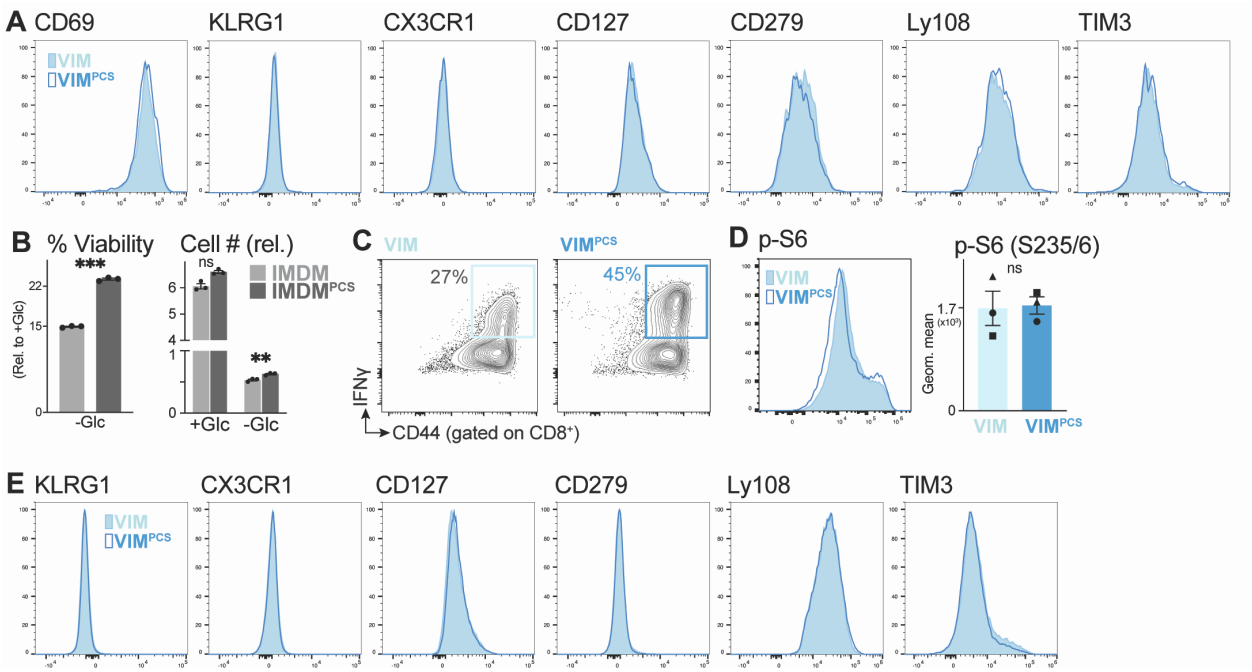

Figure S4, Related to Figure 4. Physiologic carbon sources influence T cell survival and effector function.

A, Representative histograms of cell surface marker expression (CD69, KLRG1, CX3CR1, CD127, CD279/PD-1, Ly108/Slamf6, and TIM3) in $CD8^+$ T cells activated for 3 days with plate-bound anti-CD3 and -CD28 antibodies in VIM (closed) or VIM containing PCS (open) as in **Figure 4A**. **B,** Bar graphs depicting cell viability (left) or cell number (right) of activated $CD8^+$ T cells after 48 h of culture in IMDM plus IL-2 and containing (+Glc) or lacking (-Glc) glucose. Percent viability was determined using viability dye staining and calculated relative to cell viability full glucose conditions (+Glc, 5 mM) (mean±SEM, n=3/group). Cell number was expressed relative to initial cell number at day 0 (mean±SEM, n=3/group). **C,** Representative flow cytometry plot of CD44 versus intracellular IFN-γ expression for $CD8^+$ T cells activated with plate-bound anti-CD3- and anti-CD28 antibodies for 3 days in VIM or VIM plus PCS (n=3/group). The percentage of IFN-γ^+ cells in each culture is shown. **D,** Histogram of intracellular

phospho-S6 (S235/236) protein expression in $CD8^+$ T cells activated for 3 days with plate-bound anti-CD3 and -CD28 antibodies in VIM (closed) or VIM containing PCS (open) as in **Figure S4A**. The MFI of p-S6 staining from biological replicates is shown (mean±SEM; n=3/group). **E,** Representative histograms of cell surface marker expression (KLRG1, CX3CR1, CD127, CD279/PD-1, Ly108/Slamf6, and TIM3) in $CD8^+$ T cells cultured for 7 days in VIM or VIM containing PCS as in **Figure 4G**. *, $p<0.05$; **, $p<0.01$; ***, $p<0.001$; ****, $p<0.0001$; **ns**, not significant.

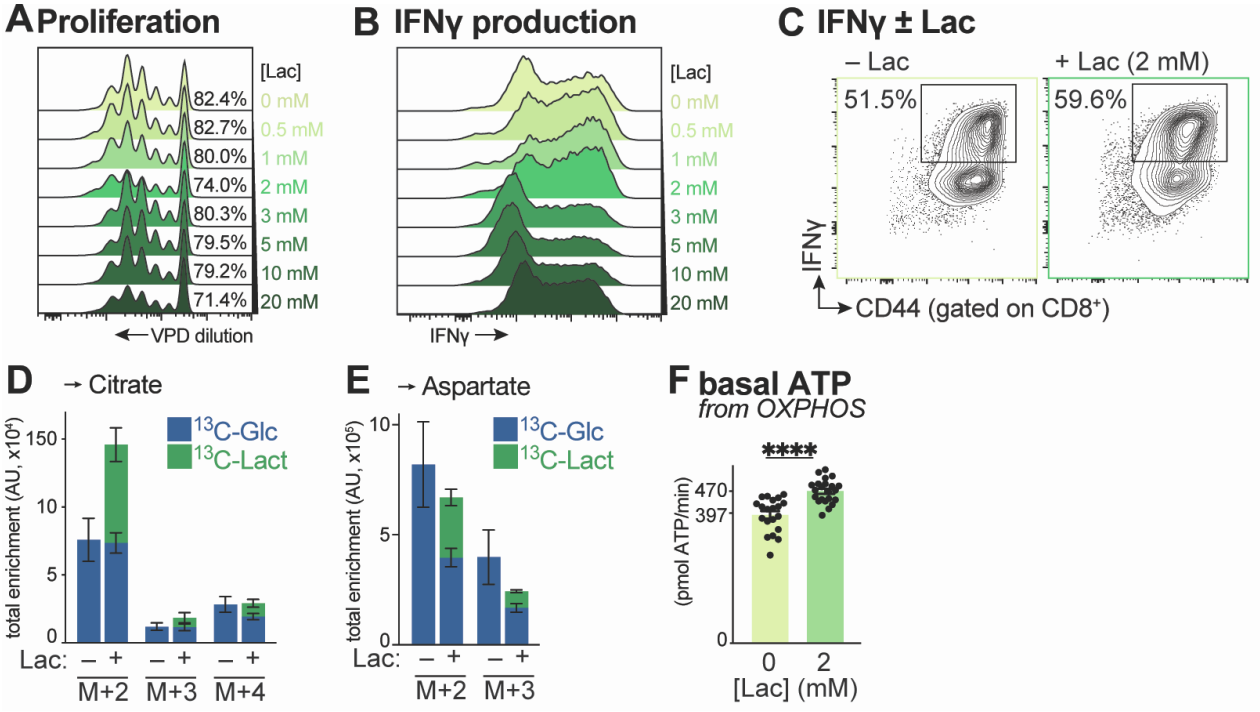

Figure S5, Related to Figure 5. Impact of exogenous lactate on CD8⁺ T cell proliferation, IFN-γ production, and metabolism.

A, Representative histograms depicting VPD dye dilution for CD8⁺ T cells activated for 3 days with anti-CD3 and -CD28 antibodies in VIM containing the indicated concentrations of sodium lactate (0, 0.5, 1, 2, 3, 5, 10, 20 mM). The percentage of CD8⁺ T cells that have undergone at least one cell division are indicated. **B,** Representative histograms depicting intracellular IFN-γ levels in CD8⁺ T cells activated as in **Figure S5A**. **C,** Representative flow cytometry plot of CD44 versus intracellular IFN-γ expression for CD8⁺ T cells cultured in VIM without (-) or containing (+) 2 mM lactate. CD8⁺ T cells were activated as in **Figure S5A**.The percentage of IFN-γ⁺ cells in each culture is shown. **D–E,** Bar graphs corresponding to **Figure 5B–C** depicting total abundance of [U-^{13}C]-glucose (blue) and [U-^{13}C]-lactate (green) labeling into (**D**) citrate (M+2–4 isotopologues) or (**E**) aspartate (M+2–3 isotopologues) in activated CD8⁺ T

cells cultured in VIM lacking (-) or containing (+) 2 mM lactate (mean±SEM, n=3/sample). **F,** Bar graph of basal OXPHOS ATP production rates for in vitro-activated $CD8^+$ T cells cultured with 0 or 2 mM lactate as in **Figure 5G** (mean±SD, n=20–22). *, $p<0.05$; **, $p<0.01$; ***, $p<0.001$; ****, $p<0.0001$; **ns**, not significant.

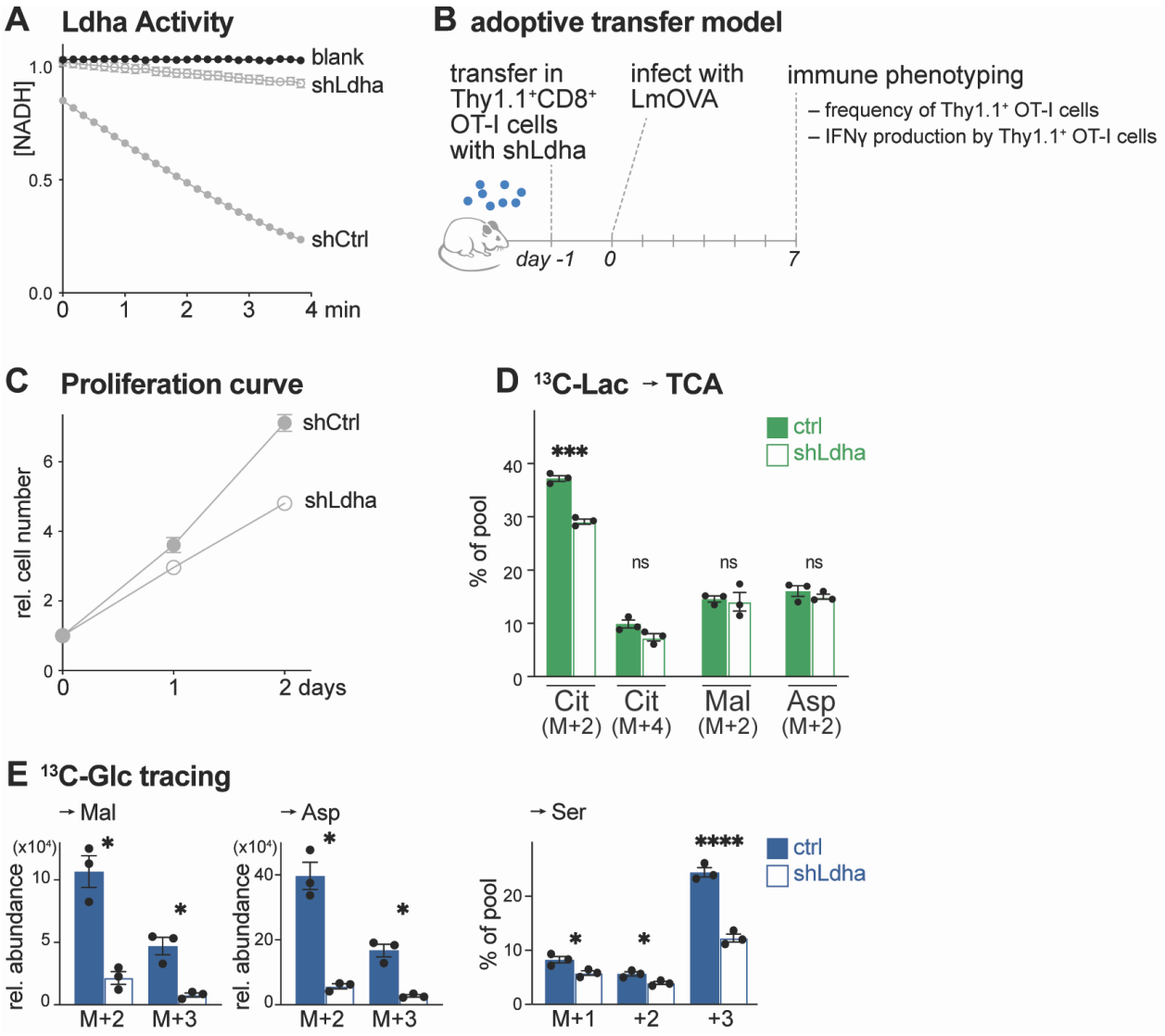

Figure S6, Related to Figure 6. Validation of Ldha silencing in CD8⁺ T cells.

A, Line graph depicting Ldh activity (via Ldh-specific NADH consumption) in cellular extracts from CD8⁺ T cells expressing control (shCtrl) or *Ldha*-targeting (sh*Ldha*) shRNAs. Blank samples containing no cellular extract were used to assess background NADH degradation. **B,** Graphic depicting adoptive transfer and *LmOVA* infection model used in **Figure 6E–F**. **C,** Line graph depicting proliferation of CD8⁺ T cells expressing control (shCtrl) or *Ldha*-targeting (sh*Ldha*) shRNAs. CD8⁺ T cells were activated for 3 days with anti-CD3 and -CD28 antibodies in IMDM medium, then biological replicates

re-cultured starting at day 0 in IMDM containing 10% dFBS (mean±SEM, n=3/sample). **D,** Bar graphs depicting MID (% of pool) for intracellular citrate (Cit M+2 and M+4), malate (Mal M+2), and aspartate (Asp M+2) for activated control (Ctrl) or sh*Ldha*-expressing $CD8^+$ T cells cultured in VIM containing 2 mM [U-^{13}C]-lactate and 5 mM unlabeled glucose for 4 h as in **Figure 6G** (mean±SEM, n=3/sample). **E,** Bar graphs depicting relative abundance of intracellular malate (Mal M+2–3) and aspartate (Asp M+2–3) and MID (% of pool) for serine (Ser M+1–3) for activated control (Ctrl) or sh*Ldha*-expressing $CD8^+$ T cells cultured in VIM containing 5 mM [U-^{13}C]-glucose and 2 mM unlabeled lactate for 4 h as in **Figure 6H** (mean±SEM, n=3/sample). *, $p<0.05$; **, $p<0.01$; ***, $p<0.001$; ****, $p<0.0001$; **ns**, not significant.